CORROSION SCIENCE AND TECHNOLOGY, Vol.16, No.1(2017), pp.31~37
[Research Paper]
pISSN: 1598-6462 / eISSN: 2288-6524
DOI: https://doi.org/10.14773/cst.2017.16.1.31

Synergistic Effect of Molybdate and Monoethanolamine on Corrosion Inhibition of Ductile Cast Iron in Tap Water

K. T. Kim[1], H. Y. Chang[2], B. T. Lim[2], H. B. Park[2], and Y. S. Kim[1,†]

[1]*Materials Research Centre for Energy and Clean Technology, School of Materials Science and Engineering, Andong National University, 1375 Gyeongdongro, Andong 36729, Korea*

[2]*Power Engineering Research Institute, KEPCO Engineering & Construction Company, 269, Hyeoksinro, Gimcheon, Gyeongbuk, 39660, Korea*

(Received December 22, 2016; Revised February 15, 2017; Accepted February 15, 2017)

A synergistic effect was observed in the combination of nitrite and ethanolamines. Ethanolamine is one of the representative organic corrosion inhibitors and can be categorized as adsorption type. However, nitrosamines can form when amines mix with sodium nitrite. Since nitrosamine is a carcinogen, the co-addition of nitrite and ethanolamine will be not practical, and thus, a non-toxic combination of inhibitors shall be needed. In order to maximize the effect of monoethanolamine, we focused on the addition of molybdate. Molybdate has been used to alternate the addition of chromate, but it showed insufficient oxidizing power relative to corrosion inhibitors. This work evaluated the synergistic effect of the co-addition of molybdate and monoethanolamine, and its corrosion mechanism was elucidated. A high concentration of molybdate or monoethanolamine was needed to inhibit the corrosion of ductile cast iron in tap water, but in the case of the co-addition of molybdate and monoethanolamine, a synergistic effect was observed. This synergistic effect could be attributed to the molybdate that partly oxidizes the metallic surface and the monoethanolamine that is simultaneously adsorbed on the graphite surface. This adsorbed layer then acts as the barrier layer that mitigates galvanic corrosion between the graphite and the matrix.

Keywords: *ductile cast iron, corrosion inhibitor, molybdate, ethanolamine, synergistic effect*

1. Introduction

In general, several corrosion inhibitors have been used to prevent the inner corrosion of pipes. The inhibiting effects depend upon the materials used, corrosion environment, and temperature etc. Corrosion inhibitors can be divided into anodic passivating, cathodic precipitation, and adsorption organic inhibitors [1]; Anodic inhibitors increase anodic polarization to the critical protection potential of the metal or alloys. They are called passivating inhibitors because they drastically decrease the corrosion current. Cathodic precipitation inhibitors decrease the corrosion rate by increasing the cathodic polarization overvoltage (hydrogen and oxygen reduction). Thick deposits form in the presence of these inhibitors, and decrease depolarizer diffusion to the metal surface, inhibiting the cathodic reaction and corrosion. Organic corrosion inhibitors contain sulfur, nitrogen, or oxygen atoms and organic heterocyclic compounds containing polar groups [2-6]. These compounds adsorb and form a covalent bond on the metal surface [7]. Organic inhibitors cover the entire surface area of the corrosion metal with a thick film consisting of several monolayers and change the structure of the double layer at the metal interface, decreasing the depolarization rate. They may also act as a barrier film by blocking anodic and cathodic active sites or decreasing the electroactive species transport rate to or from the metal surface [7].

Nitrite, which is one of the representative anodic inhibitors, inhibits corrosion by forming a Fe_2O_3 oxide film on the metal surface [8-15]. However, to inhibit the corrosion of ductile cast iron (DCI) in tap water, the nitrite is necessary at 100 kppm [16]. This is not industrially practical or economical. Nevertheless, when two kinds of corrosion inhibitors co-exist, a synergistic effect is achieved. When a film forming inhibitor and an adsorption type inhibitor were co-existed, a synergistic effect of them has been reported [17-20].

† Corresponding author: yikim@anu.ac.kr

Table 1 Chemical composition of the experimental alloy

Material	Chemical composition, wt%									
	C	Mn	P	S	Si	Cu	Mo	Ni	V	Fe
Ductile Cast Iron (DCI)*	4.008	0.173	0.022	0.026	1.528	0.023	0.028	0.059	0.016	bal.

*KS D4311

Recently, K. T. Kim and co-workers reported that this synergistic effect was observed in the combination of nitrite and ethanolamines (Monoethanolamine, MEA); Nitrite 1k ppm + MEA 1k ppm [21]. Ethanolamine is one of the representative organic corrosion inhibitors and is also one of the adsorption types. However, when amines mix with sodium nitrite, carcinogenic nitrosamines can be formed as follows;

Since this nitrosamine is one of the carcinogens, adding both nitrite and ethanolamine will be not practical and therefore a non-toxic combination of inhibitors is needed. In this work, in order to maximize the effect of monoethanolamine, we focused on the addition of molybdate [22-26]. Molybdate has been used as an alternative to adding chromate, but it shows the insufficient oxidizing power among the corrosion inhibitors. On the other hand, the synergistic effect of molybdate and organic inhibitors has been reported, but its inhibiting mechanism was not clear [25]. This work evaluated the synergistic effect of adding molybdate and monoethanolamine and its corrosion mechanism was elucidated.

2. Experimental Procedure

2.1 Materials and corrosion environments

Ductile cast iron DCI, KS D4311 [27] was used in this work. Table 1 shows the chemical composition of the experimental alloy. The test solution was a tap water with or without inhibitors. Molybdate (as Na_2MoO_4, MD) and monoethanolamine (MEA) were added in concentrations of the order of ppm.

2.2 Corrosion tests

Immersion Corrosion Test: A specimen was cut to a size of 20 × 20 × 5 mm and each surface of this specimen was ground using #120 SiC paper. Immersion tests were conducted in 500 mL glass flask containing stagnant solution. After performing the immersion test, each specimen was cleaned with acetone and alcohol. Then, this specimen was dried. Finally, the corrosion rate of this specimen was determined.

Electrochemical Tests: Specimens were cut to a size of 20 × 20 mm. After connecting these specimens in an electrical circuit, they were epoxy-mounted. Then, the surface of these specimens was ground using #600 SiC paper. Finally, these specimens were coated with epoxy resin, except an area of 1cm^2. A polarization test was performed using a potentiostat (DC105, Gamry Instruments), the reference electrode was a saturated calomel electrode, and the counter electrode was Pt wire. The test solution was deaerated using nitrogen gas: this gas was purged at a rate of 200 mL/min into the solution for 30min. The scanning rate was 0.33 mV/sec. In order to measure the AC impedance, the specimens were ground using #2,000 SiC paper. Then, these specimens were polished using a diamond paste (its diameter was 3 μm). The test solution was same as that used in polarization test. To measure AC impedance, we used an electrochemical analyser (EIS 300, Gamry Instruments). Before measuring AC impedance, passivation was performed on DCI at +200 mV and 0 mV(SCE) for 30 min. AC impedance was measured ranging from 10 kHz to 0.01 Hz and the AC voltage amplitude was 10 mV. Thereafter, a Mott-Schottky plot was constructed to determine the semi-conductive properties of the passive film. The specimen preparation was the same as that used in the measurement of AC impedance, and the DC amplitude was 10 mV (peak-to-peak) at 1,580 Hz of AC frequency [28]. The capacitance was measured at a scan rate of 50 mV/sec: the potential was varied between +1V(SCE) to -1V(SCE).

Surface Analysis; The specimen was cut to a size of 20 × 20 × 5 mm, and it was ground with #2000 SiC paper. Thereafter, it was polished with a diamond paste, which was 3 μm in diameter. Finally, the specimen was cleaned with alcohol using an ultrasonic cleaner. DCI was oxidized or in 1 kppm, 10 kppm, 100 kppm MEA or MD, and 1 kppm MD + 0.5, 1, 1.5 kppm MEA respectively. The immersion process was carried out for 72 h. In addition, an electron probe micro analyzer (EPMA, EPMA-1600, 15KV) was used to identify the elemental distribution of passivated surface.

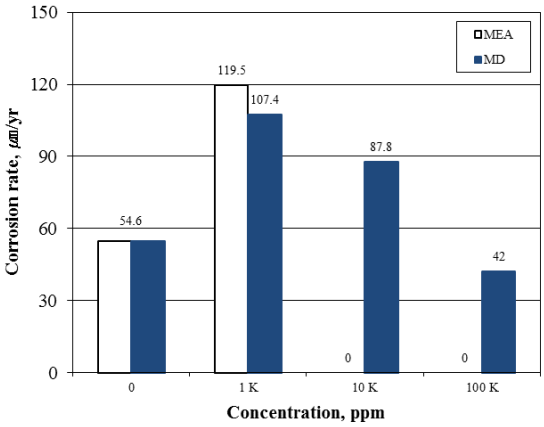

Fig. 1 Effect of single addition of corrosion inhibitor on the corrosion rates of DCI (25 ℃ tap water + x ppm corrosion inhibitor).

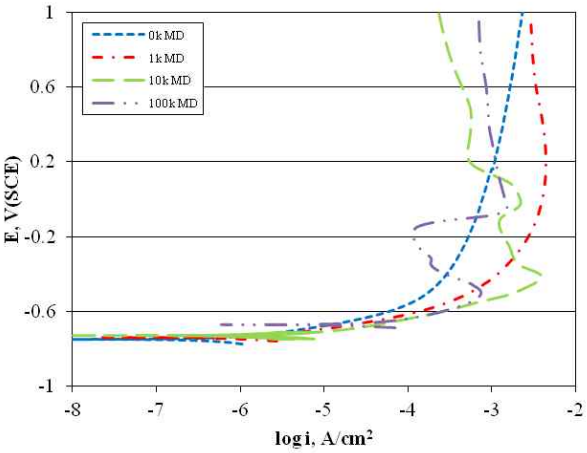

(a)

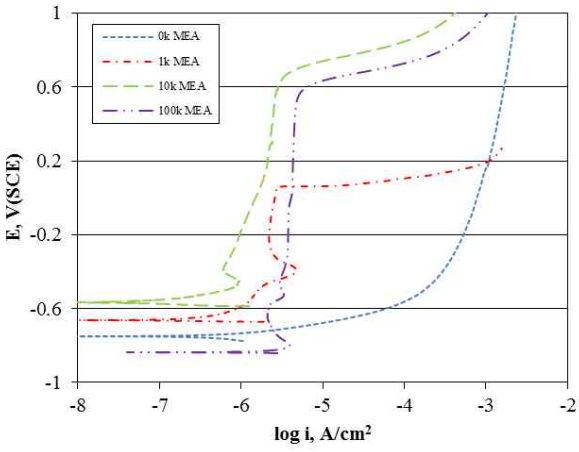

(b)

Fig. 2 Effect of single added corrosion inhibitors on anodic polarization curve of DCI (25 ℃ deaerated tap water + x ppm corrosion inhibitor); (a) MD (Molybdate), (b) M (MEA).

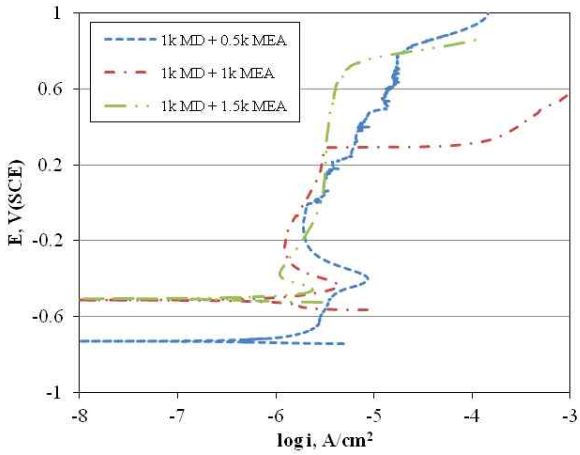

(a)

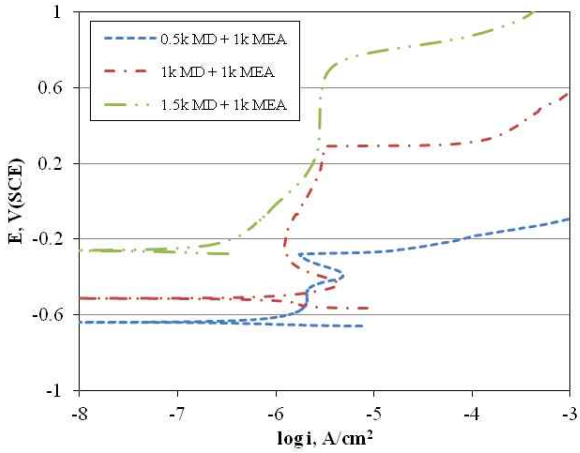

(b)

Fig. 3 Effect of mixed addition of corrosion inhibitors on anodic polarization curve of DCI (deaerated tap water + x ppm MD + 1k ppm M at 25 ℃); (a) 1k ppm MD + x ppm M, (b) x ppm MD + 1k ppm M.

3. Results

In order to evaluate the effect of a single molybdate or monoethanolamine addition, chemical immersion and electrochemical tests were performed. Fig. 1 shows the effect of a single addition of corrosion inhibitor on the corrosion rates of DCI. Test solutions were tap water + x ppm corrosion inhibitor at 25 ℃ and the samples were immersed for 72 h. In the case of single molybdate addition, the corrosion of DCI couldn't be inhibited at a very high concentration of 100 kppm. However, in the case of single monoethanolamine addition, its corrosion was inhibited from 10 kppm to 100 kppm. This high corrosion rate in a relatively low concentration of corrosion inhibitors was due to the small anode and large cathode because the whole surface of the sample was not covered

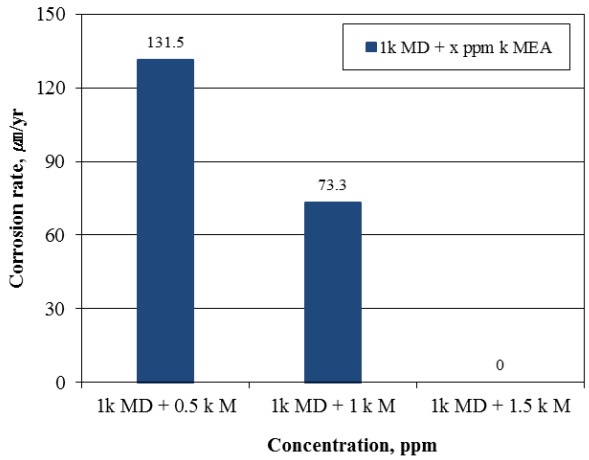

Fig. 4 Effect of co-addition of corrosion inhibitors on the corrosion rates of DCI (25 ℃ tap water + x ppm corrosion inhibitor).

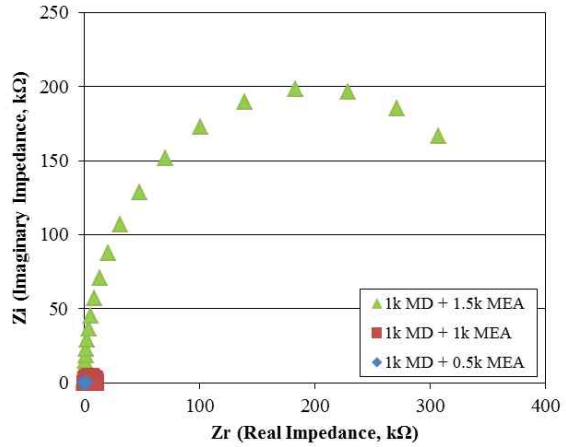

(a)

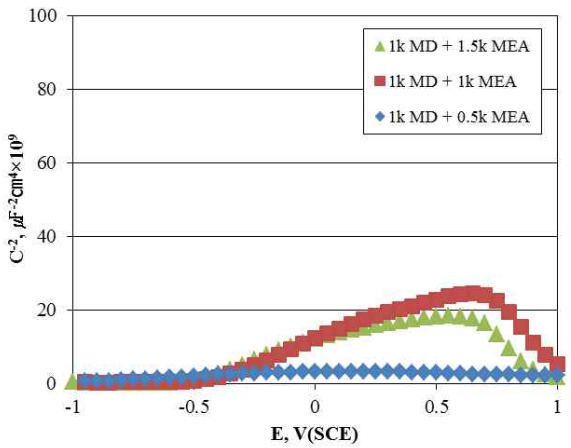

(b)

Fig. 5 Effect of corrosion inhibitors on AC impedance and Mott-Schottky of the passive film formed at 0 V(SCE) in deaerated tap water at 30 ℃; (a) Nyquist plot, (b) Mott-Schottky plot.

and passivated [16].

Fig. 2 shows the effect of a single added corrosion inhibitors on the anodic polarization curve of DCI, and the test solution was deaerated tap water + x ppm corrosion inhibitor at 25 °C. Effect of the molybdate addition is shown in Fig. 2a. However, even the 100 kppm molybdate couldn't form the good passivation of DCI. However, in the case of the MEA addition shown in Fig. 2b, 10 kppm and 100 kppm MEA additions can build up a good passive film. As reported elsewhere [21], in the case of 10 kppm MEA addition, polarization resistance measured by AC impedance was 493.6 kΩ and the passive film showed the weak n-type's semiconductive properties. But 100 kppm molybdate addition couldn't form the passivation and therefore the Mott-Schottky plot was not performed. As described the above, in the case of single molybdate or monoethanolamine additions, a very high concentration of inhibitors was needed to protect the corrosion of ductile cast iron in a tap water.

Fig. 3 reveals the effect of adding corrosion inhibitors on an anodic polarization curve of DCI. The test solution was a deaerated tap water + x ppm MD + 1k ppm M at 25 °C. When a concentration of molybdate is constant at 1 kppm, the low concentration of MEA forms a good passive film as shown in Fig. 3a. In additon, when a concentration of monoethanolamine is constant at 1 kppm, the low concentration of molybdate forms the good passive film as shown in Fig. 3b. This means that the co-addition of 2,500 ppm is sufficient for the passivation of DCI in a tap water.

Therefore, in order to verify the synergistic effect of adding both molybdate and monoethanolamine, a chemical immersion test was performed as shown in Fig.4. Fig. 4 shows the effect of co-addition of corrosion inhibitors on the corrosion rates of DCI. The test solution was a tap water + x ppm corrosion inhibitor at 25 °C.

4. Discussion

As described the above, the co-addition of 2,500 ppm completely inhibited the corrosion of DCI in a tap water and therefore the synergistic effect was verified in a chemical or electrochemical tests. Where does the synergistic effect come from? We discussed this on the basis of polarization resistance, semiconductive properties, and the elemental distribution on the surface. Fig. 5 shows the effect of corrosion inhibitors on (a) AC impedance and (b) the Mott-Schottky of the passive film formed at 0 V(SCE) in deaerated tap water at 30 °C. Co-addition less than 2,000 ppm couldn't show the polarization resistance but the concentration of 1 kppm molybdate + 1.5 kppm MEA

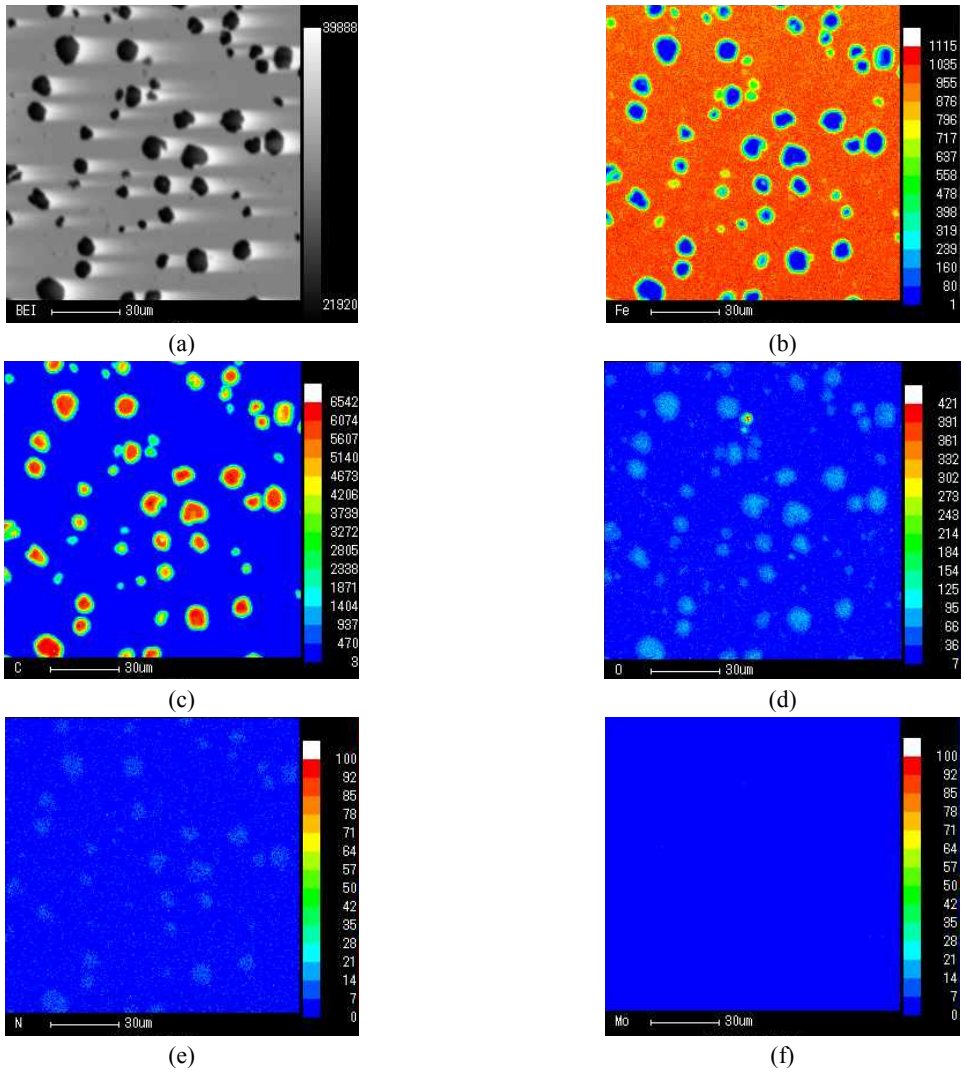

Fig. 6 Elemental distribution analyzed by EPMA on the surface of DCI, which was passivated for 72 h in tap water with 100 kppm MD addition at room temperature. (a) SEM image, (b) Fe, (c) C, (d) O, (e) N, (f) Mo.

addition reveals the good polarization resistance (Rp; 399.1 kΩ) as shown in Fig. 5a. In addition, the semiconductive properties were not observed at a concentration of 1 kppm molybdate + 0.5 kppm MEA. However, increasing the mixed concentration reveals the weak n-type semiconductive properties. It is noted that co-addition of an optimum concentration over a critical value built up the passive film with its resistance and semiconductive properties.

As shown in Fig. 1, a very high concentration of single molybdate addition couldn't inhibit the corrosion of DCI and its corrosion rate was 42 μm/year. Fig. 6 depicts the elemental distribution analysed by EPMA on the surface of DCI. This was passivated for 72 h in tap water with 100 kppm MD addition at room temperature. Fig. 6a shows the severely corroded surface appearance. A large amount of oxygen was detected on the surface as shown in Fig. 6d but this reveals the oxygen in the corrosion product. On the other hands, molybdenum was segregated partly, meaning that the added molybdate couldn't oxidize uniformly on the whole surface. K. T. Kim *et al*. [21] already reported that oxygen and nitrogen, in the case of 100 kppm MEA addition, adsorbed locally on the spherodized graphite area. On the other hands, Fig. 7 reveals the elemental distribution analysed by EPMA on the surface of DCI. This was passivated for 72 h in tap water with 1 kppm MD + 1 kppm MEA addition at room temperature. Clean surface and spherodized graphite can be confirmed in Fig. 7a. Not like Fig. 6, Fe was not present in the graphite area but carbon, oxygen, and nitrogen were enriched on the graphite areas. However, Mo was well distributed on the surface. As reported earlier for the

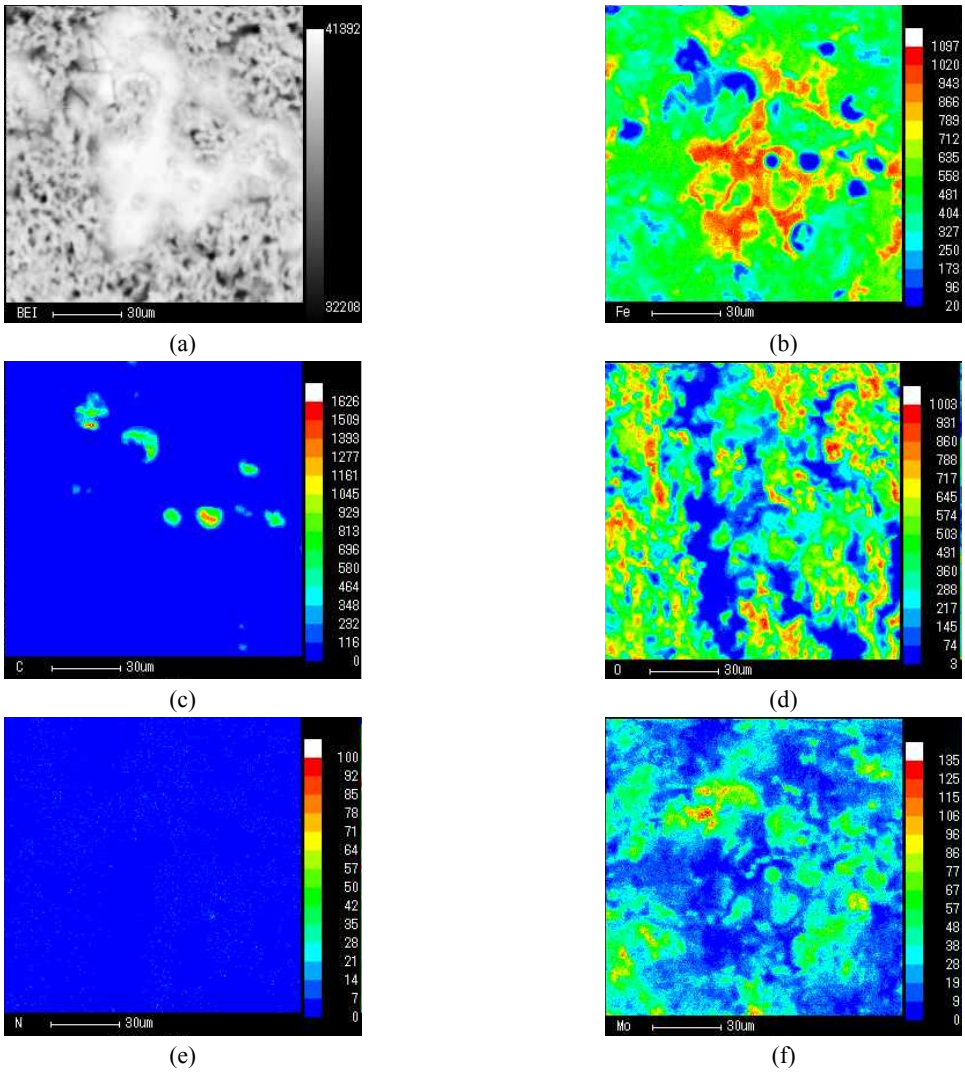

Fig. 7 Elemental distribution analysed by EPMA on the surface of DCI, which was passivated for 72 h in tap water with 1 kppm MD + 1 kppm MEA addition at room temperature. (a) SEM image, (b) Fe, (c) C, (d) O, (e) N, (f) Mo.

co-addition of nitrite and triethanolamine [29], owing to the synergistic effect of nitrite and TEA, there was effective inhibition of DCI corrosion in tap water; The inhibitory effect was *ca*. 30 times more effective than that witnessed with single additions; This synergistic effect occurs by the following process; Among the two inhibitors, nitrite oxidizes the metallic surface. On the other hand, TEA gets adsorbed simultaneously at the graphite surface. This adsorbed layer acts as a barrier layer that mitigates the galvanic corrosion between graphite and matrix. Finally, a synergistic effect is achieved. In summary, in the case of co-addition of molybdate and monoethanolamine, a synergistic effect that inhibits the corrosion of DCI in a tap water was observed. It can be considered that molybdate oxidizes the metallic surface partly and monoethanolamine is adsorbed simultaneously at the graphite surface. This adsorbed layer acts as the barrier layer that mitigates the galvanic corrosion between graphite and the matrix.

5. Conclusions

1) High concentration of molybdate or monoethanolamine was needed to inhibit the corrosion of DCI in a tap water but in the case of co-addition of molybdate and monoethanolamine, synergistic effect was observed.
2) This synergistic effect was attributed to the molybdate that partly oxidizes the metallic surface and the monoethanolamine adsorbed simultaneously on the graphite surface. This adsorbed layer acts as the barrier layer that mitigates the galvanic corrosion between graphite and the matrix.

Acknowledgments

This work was supported by the Nuclear Power Core Technology Development Program of the Korea Institute of Energy Technology Evaluation and Planning (KETEP) granted financial resource from the Ministry of Trade, Industry & Energy, Republic of Korea (No. 20131520000100).

References

1. B. N. Popov, *Corrosion Engineering; Principles and solved problems*, p.583, Elsevier Publication, Waltham, USA (2015).
2. S. W. Dean Jr., R. Dervy, and G. T. Vondembussche, *Mater. Perform.*, **20**, 47 (1981).
3. L. Wang, *Corros. Sci.*, **43**, 2281 (2001).
4. M. A. Quraishi and R. Sadar, *Corrosion*, **58**, 748 (2002).
5. F. Bentiss, M. Lebrini, H. Vezin, and M. Lagrenee, *Mater. Chem. Phys.*, **87**, 18 (2004).
6. E. A. Noor, *Corros. Sci*., **47**, 33 (2004).
7. G. Trabanelli, *Corrosion Inhibitors*, F. Mansfield ed., p.28, Marcel Dekker, New York (1970).
8. M. Cohen, *J. Electrochem. Soc.,* **93**, 26 (1948).
9. R. Pyke and M. Cohen, *J. Electrochem. Soc.,* **93**, 63 (1948).
10. M. Cohen, R. Pyke, and P. Marier, *J. Electrochem. Soc.*, **96**, 254 (1949).
11. S. Matsuda and H. H. Uhlig, *J. Electrochem. Soc.,* **111**, 156 (1964).
12. W. D. Robertson, *J. Electrochem. Soc.*, **98**, 94 (1951).
13. M. J. Pryor and M. Cohen, *J. Electrochem. Soc.,* **100**, 203 (1953).
14. S. Karim, C. M. Mustafa, M. Assaduzzaman, and M. Islam, *Chem. Eng. Res. Bull.,* **14**, 87 (2010).
15. Y. T. Horng and Y. L. Tsai, *Corros. Sci. Tech.*, **2**, 233 (2003).
16. K. T. Kim, H. W. Kim, H. Y. Chang, B. T. Lim, H. B. Park, and Y. S. Kim, *Adv. Mater. Sci. Eng.*, Article ID 408138 (2015).
17. I. Carrillo, B. Valdez, R. Zlatev, M. Stoytcheva, M. Carrillo, and R. Bäßler, *Inter. J. Electrochem. Sci.*, **7**, 8688 (2012).
18. J. O. Okeniyi, A. P. I. Popoola, C. A. Loto, O. A. Omotosho, S. O. Okpala, and I. J. Ambrose, *Adv. Mater. Sci. Eng.*, Article ID 540395 (2015).
19. A. M. Ridhwan, A. A. Rahim, and A. M. Shah, *Inter. J. Electrochem. Sci.*, **7**, 8091 (2012).
20. M. Vishnudevan, *Iran. J. Mater. Sci. Eng.,* **9**, 17 (2012).
21. K. T. Kim, H. Y. Chang, B. T. Lim, H. B. Park, and Y. S. Kim, *Corros. Sci. Tech*., **15**, 171 (2016).
22. E. A. Lizlovs, *Corrosion,* **32**, 263 (1976).
23. D. R. Robitaile, *Mater. Perform.*, **15**, 40 (1976).
24. J. Jefferies, *Mater. Perform.*, **31**, 50 (1992).
25. A. M. Shams El Din and L. Wang, *Desalination*, **107**, 29 (1996).
26. M. Guannan, L. Xianghong, Q. Qing, and Z. Jun, *Corros. Sci*., **48**, 445 (2006).
27. KS D 4311, Ductile Iron Pipes, Korean Standards Association (2010).
28. D. D. Macdonald, *J. Electrochem. Soc.*, **139**, 3434 (1992).
29. K. T. Kim, H. Y. Chang, B. T. Lim, H. B. Park, and Y. S. Kim, *Adv. Mater. Sci. Eng.,* Article ID 4935602 (2016).